

## Highly porous hydroxyapatite ceramics for engineering applications

Hrvoje Ivankovic<sup>1,a</sup>, Sebastijan Orlic<sup>1,b</sup>, Dajana Kranzelic<sup>1,c</sup> and Emilija Tkalcec<sup>1,d</sup>

<sup>1</sup> University of Zagreb, Faculty of Chemical Engineering and Technology, Zagreb, Croatia

<sup>a</sup>hivan@fkit.hr, <sup>b</sup>sorlic@fkit.hr, <sup>c</sup>dkranzelic@fkit.hr, <sup>d</sup>etkalcec@fkit.hr

**Keywords:** Hydroxyapatite, Cuttlefish bone, DTA-TG-EGA-FTIR, Microstructure

**Abstract** Highly porous hydroxyapatite ( $\text{Ca}_{10}(\text{PO}_4)_6(\text{OH})_2$ , HA) was prepared through hydrothermal (HT) transformation of aragonitic cuttlefish bones (*Seppia Officinalis* L. Adriatic Sea) in the temperature range from 140°C to 220°C for 20 minutes to 48 hours. Mechanism of hydrothermal transformation of bones was investigated by DTA/TG analyzer coupled online with FTIR spectrometric gas cell equipment (DTA-TG-EGA-FTIR analysis), X-ray diffraction analysis (XRD) and scanning electron microscopy (SEM). DTA-TG-EGA-FTIR analysis have shown the release of  $\text{CO}_2$  at about 400°C, 680°C and 990°C. The first release could be attributed to organics not completely removed from the heat treated bones, and the second release to decomposition of unconverted aragonite, whereas, the third one could be attributed to  $\text{CO}_3^{2-}$  groups incorporated in the structure of HA. The interconnecting porous morphology of the starting material (aragonite) was maintained during the HT treatment. The formation of dandelion-like HA spheres with diameter from 3 to 8  $\mu\text{m}$  were observed, which further transformed into nanoplates and nanorods with an average diameter of about 200-300 nm and an average length of about 8-10  $\mu\text{m}$ .

### 1. Introduction

Hydroxyapatite (HA) is being extensively used as bone grafting material in hard tissue implants and as material for bone-tissue engineering applications, due to its excellent biocompatibility and osteoconductivity [1]. Non-medical applications of porous HA ceramics include packing media for column chromatography, gas sensors, catalyst and host materials [2]. The most of the synthetic HA is stoichiometric with chemical composition  $\text{Ca}_{10}(\text{PO}_4)_6(\text{OH})_2$ . By contrast, HA prepared from natural sources, which primarily include corals, nacles, animal bones, exoskeletons etc. is non stoichiometric, and have other ions incorporated, mainly  $\text{CO}_3^{2-}$ , trace of  $\text{Na}^+$ ,  $\text{Mg}^{2+}$ ,  $\text{Fe}^{2+}$ ,  $\text{F}^-$ ,  $\text{Cl}^-$  [3].  $\text{CO}_3^{2-}$  containing HA has gained much attention as it can be more easily resorbed by the living cells in comparison with stoichiometric HA, and therefore it leads to faster bone regeneration.  $\text{CO}_3^{2-}$  can be substituted for either  $\text{OH}^-$  (A-type) or  $\text{PO}_4^{3-}$  (B-type) groups in the structure of hydroxyapatite. Sometimes, both A-type and B-type substitutions can also occur [4]. Several attempts to convert natural aragonite structures (e.g. corals, nacles, etc.) hydrothermally (HT) to hydroxyapatite have been reported [5-9]. The reaction sequences in hydrothermal systems are complex and in most cases the information regarding the course of reactions is only partial. Various mechanisms of transformation of  $\text{CaCO}_3$  into HA are assumed in literature. The ability of fast transformation of natural aragonitic ( $\text{CaCO}_3$ ) structure into HA, even at room temperature, has been shown by Ni et al. [10]. Rocha et al. [7-9] were the first one who performed the hydrothermal

transformation of aragonitic cuttlefish bones into HA. The inorganic part of cuttlefish bone (also called cuttlebone) is a lamellar mineralized porous structure of aragonite. Its highly channeled structure favors the diffusion of the reaction solution towards the aragonite and its fast transformation into HA. Zaremba et al. [11] studying the aragonite transformation in gastropod (abalone) nacles suggested dissolution-recrystallization mechanism of the HA growth, whereas Yoshimura et al. [12], proposed dissolution-precipitation mechanism followed by nucleation and growth of HA on the surface of calcite ( $\text{CaCO}_3$ ). According to Jinawath et al. [13], aragonite in porites was initially transformed into intermediate  $\text{CaHPO}_4$  (DCPA) at  $\text{pH} \sim 2-4$ , which at  $\text{pH} > 6$  transformed into HA. The authors also proposed dissolution-recrystallization mechanism as driving force for hydroxyapatite growth.

The aim of this work was: to study the transformation mechanism of aragonitic cuttlefish bones into HA in the dependence of temperature and time of hydrothermal treatment. Incorporation of  $\text{CO}_3^{2-}$  groups into HA structure has been studied by DTA-TG-EGA-FTIR analysis.

## 2. Materials and methods

The starting materials were pieces of native cuttlefish bones ( $\sim 2\text{cm}^3$ ), *Sepia Officinalis L.*, from the Adriatic Sea, heated at  $350^\circ\text{C}$  for 3 h, to remove the organic part of cuttlefish bones. The bones were poured with the required volume of an aqueous solution of 0.6 M  $\text{NH}_4\text{H}_2\text{PO}_4$  ( $\text{Ca/P}=1.67$ ) in teflon lined stainless steel pressure vessel and sealed from  $140^\circ\text{C}$  to  $220^\circ\text{C}$  in the step of  $20^\circ\text{C}$  for various times (20 minutes to 48 hours) in the electric furnace. The converted HA was washed with boiling water and dried at  $110^\circ\text{C}$  for further characterization. The conversion of HT transformation was followed by X-ray diffraction analysis (Philips PW 1820 counter diffractometer with  $\text{Cu K}\alpha$  radiation). To quantify the HA transformed by hydrothermal treatment, Rietveld structure refinement approach was used [14]. Fourier transform infrared spectra (FTIR) were performed by attenuated total reflectance (ATR) spectroscopy for solids with a diamond crystal. DTA-TG-EGA-FTIR analysis were monitored on DTA/TG analyzer Netzsch STA 409 with an online coupled Fourier transform infrared attenuated total reflectance spectrometer (ATR-FTIR Bruker Vertex 70). The samples were heated in DTA from room temperature to  $1350^\circ\text{C}$  with a heating rate of  $10^\circ\text{C min}^{-1}$  in flowing nitrogen ( $30\text{ cm}^3\text{ min}^{-1}$ ). DTA was coupled to FTIR via heated transfer line connected to an interface that consisted of gas cell heated up to  $200^\circ\text{C}$  to prevent condensation on the windows. The FTIR spectrometer acquired 996 complete IR spectra with measuring resolution of  $8\text{ cm}^{-1}$  and iteration was performed for 32 times in the range  $4000\text{--}650\text{ cm}^{-1}$ .

### 3. Results and discussion

The conversion of aragonite was followed by quantitative XRD analysis. XRD patterns of the samples HT treated for 20 minutes at various temperatures are given in Fig.1. Poorly crystallized

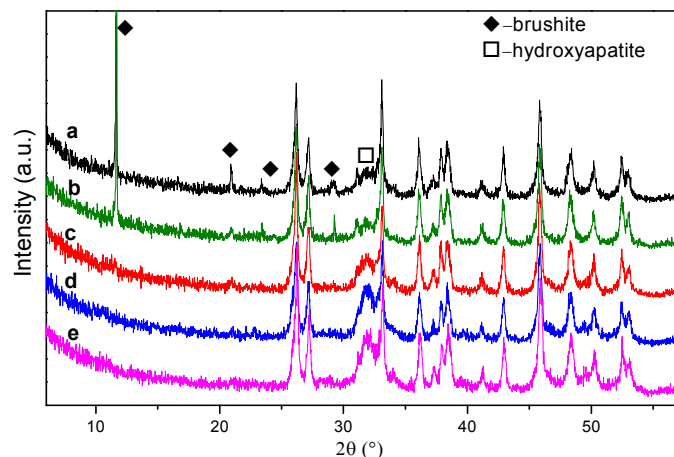


Fig.1. XRD patterns of samples HT treated at: (a)-140°C, (b)-160°C (c)-180°C, (d)-200°C and (e)-220°C for 20 minutes

hydroxyapatite and well crystalline brushite,  $\text{CaHPO}_4 \cdot 2\text{H}_2\text{O}$ , were determined in the samples heat treated at 140°C and 160°C. With the increase of HT temperature, the amount of brushite decreases, so at 180°C just discernible amount of brushite is detected, and at 200°C brushite was not observed. XRD patterns for samples HT treated at 180°C are shown in Fig.2. as an example. The sample HT treated at 180°C for 48 hours contained 95.4 wt% of HA and 4.6 wt% of untransformed aragonite, while in the sample treated at 200°C for 24 hours aragonite transformed completely into hydroxyapatite. On the other hand, the sample treated at 220°C for 24 hours contained 97.9 wt % of HA, and 2.1 wt% of untransformed aragonite, while for longer treatment time (48 h), the amount of hydroxyapatite decreased on account of monetite,  $\text{CaHPO}_4$ , which was formed in quantity of 3.2 wt %.

The FTIR spectra of HT treated samples at 180°C are given in

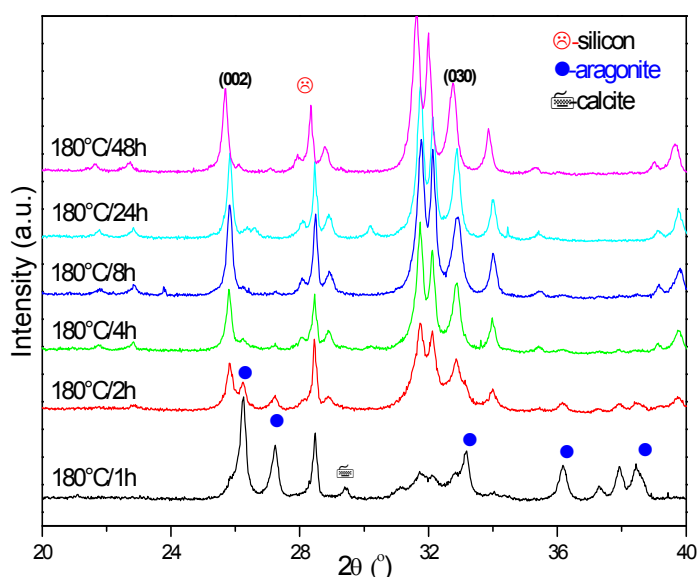


Fig.2. XRD pattern of HT samples treated at 180°C

Fig.3. The formation of HA by HT treatment is evident according to characteristic bands of  $\text{PO}_4^{3-}$  tetrahedra: ( $\nu_3$  1042 and 1088  $\text{cm}^{-1}$ ;  $\nu_4$  602 and 563  $\text{cm}^{-1}$ ;  $\nu_1$  960  $\text{cm}^{-1}$  and  $\nu_2$  470  $\text{cm}^{-1}$ ) [15]. With the increase of HT treatment time, the intensities and resolutions of  $\text{PO}_4^{3-}$  bands are increased and  $\text{OH}^-$  band at 3570  $\text{cm}^{-1}$  appears. The small intensity of  $\text{OH}^-$  bands is also characteristic for nanocrystalline biological apatites; probably because of a greater amount of

carbonate ion incorporated in HA structure [16]. Accordingly, the same explanation could be valid for our results too. In general, there are two types of  $\text{CO}_3^{2-}$  substitutions in apatites; the substitution at the  $\text{OH}^-$  site (A-type) and at the  $\text{PO}_4^{3-}$  site (B-type) [17] which is reflected on the FTIR spectra.

The broad bimodal peaks at 1412 and 1446  $\text{cm}^{-1}$  and the peak at 872  $\text{cm}^{-1}$  confirms carbonate ion in the B-site of HA structure. When the cuttlefish bone is treated at 200°C, the  $\text{OH}^-$  stretching

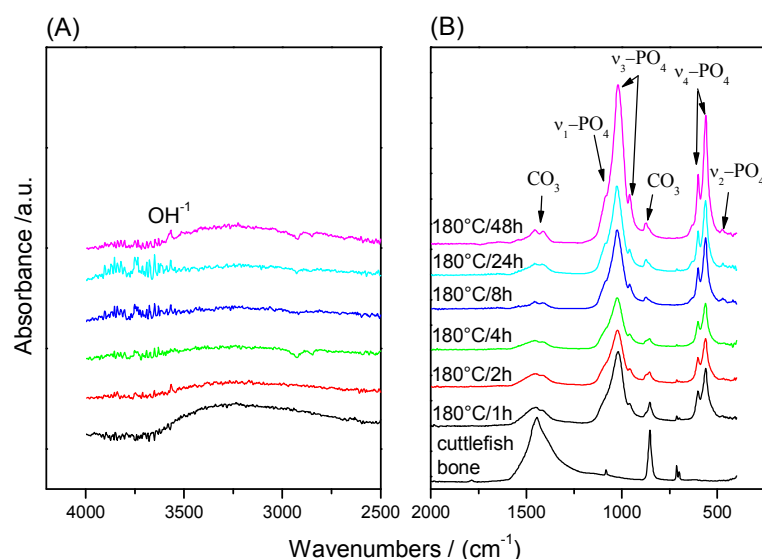


Fig.3. FTIR spectra of hydrothermally converted HA at 180°C

vibrations are visible already in the samples treated for 1 hour and became more intense with duration of HT treatment. The unconverted aragonite has been analyzed by DTA/TG analysis, and simultaneously the amount of incorporation of  $\text{CO}_3^{2-}$  in the HA structure has been followed by the *in situ* online coupled DTA-TG-EGA-FTIR system. The results obtained from DTA-TG-EGA-FTIR analysis generally are

presented as (1) a Gram-Schmidt plot, which shows information related with the total IR absorbance of the evolved components in whole spectral range; (2) a three dimensional spectra (a stacked plot) of evolved gases; and (3) IR spectra obtained at the maximum evolution rate for each decomposition stage. DTA-TG curves are shown in comparison with the Gram-Schmidt plot for the sample HT treated at 180°C (Fig. 4.). Three evolved gases regions at ~400°C, 690°C and 990°C can be distinguished on Gram-Schmidt plot characterized with the mass loss on TG curve. 3D stacked plot, and the IR spectra of evolved gas in the region between 320°C and 1200°C suggest that  $\text{CO}_2$  is the sole gas evolved during the DTA-TG-EGA-FTIR analysis.

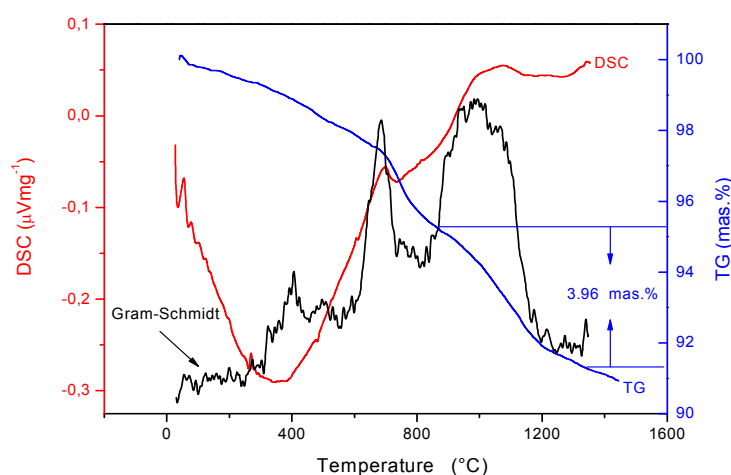


Fig.4. DTA/TG scans and Gram-Schmidt plot of HT treated sample at 180°C for 24 h

The first release of  $\text{CO}_2$  at about 400°C could be attributed to oxidation of organics not completely decomposed at the pretreatment of cuttlefish bone, and  $\text{CO}_2$  release at about 690°C should be attributed to decomposition of aragonite. Namely, unconverted aragonite was also

visible already in the samples treated for 1 hour and became more intense with duration of HT treatment. The unconverted aragonite has been analyzed by DTA/TG analysis, and simultaneously the amount of incorporation of  $\text{CO}_3^{2-}$  in the HA structure has been followed by the *in situ* online coupled DTA-TG-EGA-FTIR system. The results obtained from DTA-TG-EGA-FTIR analysis generally are

determined by XRD analysis. The release of gaseous  $\text{CO}_2$  between  $800^\circ\text{C}$  and  $1060^\circ\text{C}$  should be attributed to  $\text{CO}_3^{2-}$  groups incorporated in HA structure. The absorption bands at about  $2400$  and

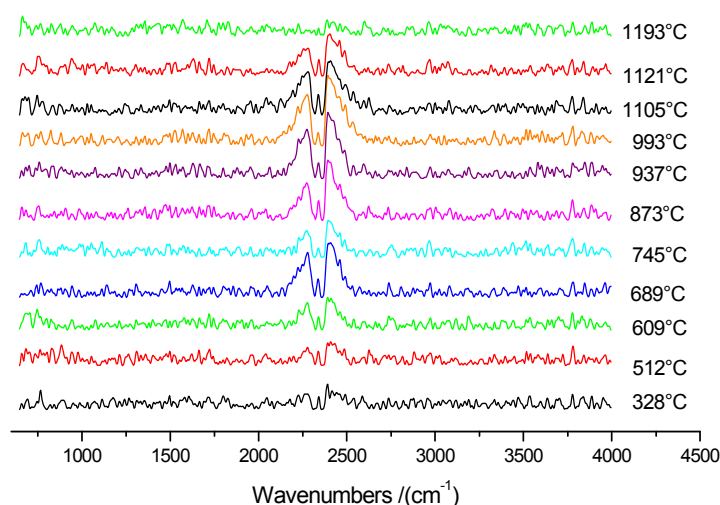


Fig.5. Evolution of gaseous species ( $\text{CO}$ ,  $\text{CO}_2$ ) from the sample HT treated at  $180^\circ\text{C}$  as observed in *in situ* DTA-TG-EGA-FTIR measurement

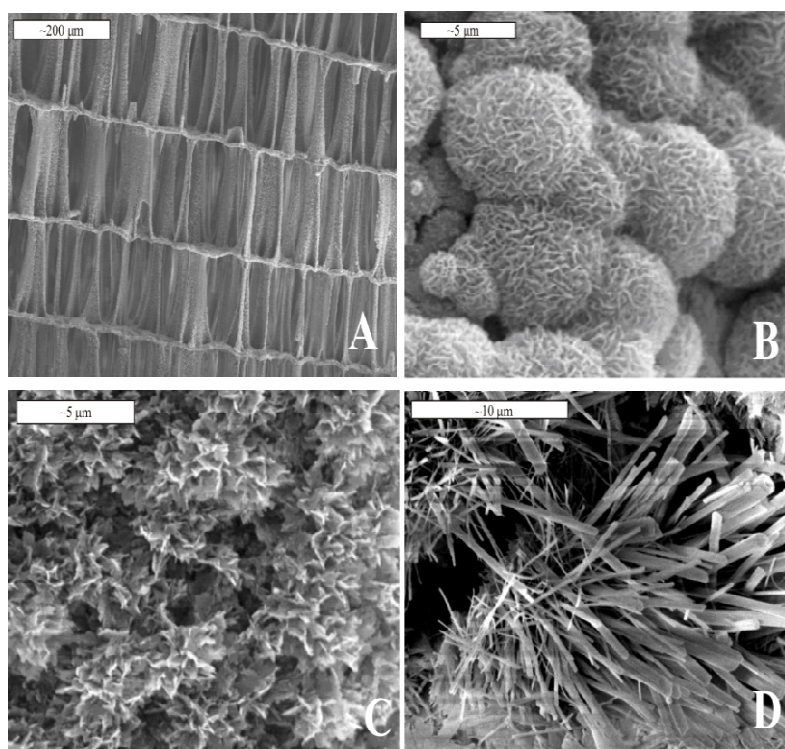


Fig.6. SEM micrographs converted cuttlefish bone at  $180^\circ\text{C}$ : a) general image, b) dandelion-like nanostructures, c) nanoplates and d) nanorods of HA.

$2270\text{ cm}^{-1}$  in Fig.5. indicate that  $\text{CO}_3^{2-}$  incorporated into HA is released at about  $1000^\circ\text{C}$ . SEM micrographs have shown that the general image of cuttlefish bones was preserved after hydrothermal treatment and the cuttlefish bones retained its form with the same channel size ( $\sim 80 \times 300\text{ }\mu\text{m}$ ). The enlarged view of transformed HA (Fig.6.) indicates the existence of many uniform, dandelion-like HA nanostructures with diameter from  $3$  to  $8\text{ }\mu\text{m}$ , formed on the surface of lamellae and pillars. With the prolonged HT treatment, the dandelion-like structures [18] are transformed into various nanostructure branches which later form radially oriented nanoplates and nanorods with an average diameter of about  $200\text{--}300\text{ nm}$  and an average length of about  $8\text{--}10\text{ }\mu\text{m}$ .

#### 4. Conclusions

Transformation of aragonitic cuttlefish bones into hydroxyapatite using hydrothermal treatment at temperatures between  $140^\circ\text{C}$  and

$220^\circ\text{C}$  for various times (1-48 h) has been investigated. In the initial reaction step at  $140^\circ\text{C}$  and  $160^\circ\text{C}$  small amount of brushite ( $\text{CaHPO}_4 \cdot 2\text{H}_2\text{O}$ ) was crystallized, due to acidic conditions of the suspension in the pressure vessel.



DTA-TG-EGA-FTIR analysis has shown that  $\text{CO}_3^{2-}$  groups incorporated into HA are released from the structure at about  $990^\circ\text{C}$ . The interconnecting porous morphology of the starting material (aragonite) was maintained during the HT treatment. Dandelion-like HA nanostructures were formed. Maintained 3D architecture of the natural cuttlefish bones offer promising alternatives for bone tissue engineering, bulk catalyst and host materials application.

### Acknowledgment

The financial support of the Ministry of Science, Education and Sports of the Republic of Croatia in the framework of the project “Bioceramic, Polymer and Composite Nanostructured Materials”, (No.125-1252970-3005) and Universidad Politecnica de Valencia, (Centro de Biomateriales) Spain is gratefully acknowledged.

### References

1. L.L. Hench, J. Wilson: Introduction to bioceramics, Singapore World Scientific; 1993.
2. K.Yamashita, T. Kazanawa: Inorganic phosphate Materials, ed. T. Kazanawa, Elsevier, Amsterdam; 1989
3. L.Z. LeGeros in P.W. Brown, B. Constantz (Eds. Hydroxyapatite and Related Materials, CRC Press, Boca Raton
4. R. Murugan, S. Ramakrishna: Acta Biomaterialia 2 (2006) 201
5. J. Hu, J.J. Russell, B. Ben Nissan, R. Vago: J. Mater. Letters (2001) 20; 85
6. K.S. Vecchio, X. Zhang, J.B. Massie, M. Wang, CW. King, Conversion of bulk seashells to biocompatible hydroxyapatite for bone implants, Acta Materialia 3 (2007) 910
7. J.H.G. Rocha, A.F. Lemos, S. Agathopoulos, P. Valério, S. Kannan, F.N. Oktar, J.M.F. Ferreira: Bone 37 (2005) 850
8. J.H.G. Rocha, A.F. Lemos, S. Agathopoulos, S. Kannan, P.Valerio, J.M.F. Ferreira: J. Biomedical Mater. Res., Part A 77A [1] (2006) 160
9. J.H.G. Rocha, AF. Lemos, S. Kannan, S. Agathopoulos, JMF. Ferreira: J. Mater. Chem. 15 [47] (2005), 5007
10. M. Ni, B.D. Ratner: Biomaterials 24 (2003) 4323
11. C.M. Zaremba, D.E. Morse, S. Mann, P.K. Hansma, G.D. Stucky: Chem. Mater. 10 (1998) 3813
12. M. Yoshimura, P. Suyaridworakun, F. Koh, F. Fujiwara, D. Pongkau, A. Ahniyaz: Mater. Sci. & Eng. C 24 (2004) 521
13. S. Jinawath, D. Polchai, M.Yoshimura: Mater. Sci. & Eng. C 22 (2002) 35
14. R.A Young, The Rietveld method International Union of Crystallography. Monographs on Crystallography, Vol 5, Oxford Press, Oxford, 1993
15. A.F. Lemos, J.H.G. Rocha, S.S.F. Quaresma, S. Kannan, S. Agathopoulos, J.M.F. Ferreira: J. Eur. Ceram. Soc. 26 (2006) 3639
16. J.D. Pasteris, B. Wopenka, J.J. Freeman, K. Rogers, E. Valsami-Jones, J.A.M. van der Houwen M.J. Silva: Biomaterials 25 (2004) 229
17. E. Landi, G. Celotti, G. A. Tampieri: J. Eur. Ceram. Soc. 23 (2003) 2931
18. J. Liu, K. Li, H. Wang, M. Zhu, H. Yan: Chem. Phys. Letters 396 (2004) 429